Parawing Technology for Spacecraft Land Landing a Progress Report

J. H. MOELLER* AND E. M. LINHART†
Northrop Corporation, Newbury Park, Calif.

This paper describes some of the significant findings of a 2½ year program conducted to investigate the suitability of the all-flexible parawing as a primary descent system for large spacecraft. The program included wind tunnel tests of small parawings and 75 aerial drop tests of 400 ft² and 4000 ft² parawings. The parawing configuration, structural arrangement and method of multistage reefing are described. Deployment data are presented to show that deployment loads could be maintained at a level of 3.0–3.5G's. *L/D* performance of the wings in free gliding flight was in the range of 2.5–2.75. However, significant modulation of *L/D* for control of glide path angle was not achieved using either tip-line or rear keel-line control. Also, the large parawings showed a susceptibility to localized canopy fabric damage during initial deployment and reefed inflation. Over-all, the program demonstrated that large parawings could be built, deployed at high speed and brought to a configuration for controlled, gliding flight. Although the program was directed toward a spacecraft recovery application, the resulting advancement in technology and the demonstrated parawing performance are considered applicable to other deceleration system requirements.

Nomenclature

b_0	=	flat pattern wing span, ft
C_D	=	drag coefficient, D/qS_w
C_L	=	lift coefficient, L/qS_W
D	=	drag
G	=	ratio of acceleration to Earth gravity
L	=	lift
l_K	=	reference keel length
l_{RK}	=	length of rear keel suspension lines
l_{RL}	=	effective reefing line length, including end attachments for noncontinuous reefing lines
l_T	=	length of tip suspension line
$(l_T/l_K)_{AVE}$	=	average tip setting—ratio of the average length of the left and right tip suspension lines to the reference keel length
q	=	dynamic pressure, psf
S_W	=	reference canopy area of parawing, ft² (equal to $0.7726\,l_K^2$)
W_D	=	descent weight, lb
W_D/S_W	=	unit canopy loading (wing loading), lb/ft²
δ_T/l_K	=	differential tip setting—ratio of difference in length of right and left tip suspension lines to reference keel length
$\dot{\psi}$	=	turn rate, deg/sec

Introduction

A DEPLOYABLE, aerodynamic deceleration device capable of controlled, gliding flight is a promising approach to the problem of providing a land landing capability for manned spacecraft. One such candidate device, the all-flexible parawing, was initially developed by the NASA Langley Research Center.[1,2] To establish the suitability of the parawing as a primary descent system for large spacecraft, a 2½ year parawing technology program was undertaken by Northrop for the NASA, Langley Research Center. The major aim of the program was to demonstrate that large parawings could be built, successfully deployed at the high-speed conditions typical for current spacecraft recovery systems, and then brought to a gliding configuration to provide controlled, stable system descent and landing. Significant technical aspects of the program included design of a reliable, multistage, parawing reefing system to provide the required low G-loads during the deployment process, and structural design of large parawings capable of withstanding high-speed deployment and subsequently providing high gliding performance. Much of the information and data presented herein were derived from investigations conducted with the large (4000 ft²) parawings. However, where pertinent, data summaries are presented showing compilations of both small and large parawing results. Also, comparisons are drawn between the gliding flight characteristics of the small parawings and the large parawings.

Although both twin keel and single keel parawing configurations were investigated in the program, only the twin keel configuration is discussed in this paper, since it proved to be a superior configuration in terms of its maximum L/D glide capability.

Large Parawing Test Specimen

Configuration

The parawing is a completely flexible flying wing. The flying shape of the wing is determined by the pressure distribution across the canopy and the tension forces in the canopy and suspension lines. No compressive load bearing structure is employed in the wing. Figure 1 shows a 4000 ft² parawing in the gliding configuration on a bomb-type test vehicle.

Figure 2 shows the flat planform layout of the large, twin keel parawing. The wing consists of a rectangular center section with two isosceles-triangle outer sections. The reference keel length l_K was 72 ft with a wing span b_0 of 110 ft and a total constructed canopy area of 4000 ft². A total

Presented as Paper 70-1187 at the AIAA Aerodynamic Deceleration Systems Conference, Dayton, Ohio, September 14–16, 1970; submitted September 30, 1970; revision received May 12, 1971. The information presented in this paper resulted from work conducted by Northrop under NASA Langley Contract NAS-7467.

Index category: Post-Entry Deceleration Systems and Flight Mechanics.

* Engineering Specialist, Ventura Div. Member AIAA.
† Engineering Specialist, Ventura Div.

of 52 suspension lines were attached to the wing canopy: 11 lines along each leading edge, 12 lines along each of the 2 keels, and 3 lines along the trailing edge of each outer section, as indicated in Fig. 2. The first large parawings built and flown had only 6 lines along each leading edge. However, structural problems encountered in deployment led to the addition of 5 more lines along each leading edge, spaced at intermediate points between the original 6 lines. To avoid renumbering existing lines, the added lines were numbered $1\frac{1}{2}$, $2\frac{1}{2}$, etc., as shown in Fig. 2.

Structural Arrangement

The structural arrangement of the large parawing is shown in Fig. 3. Figure 3 identifies the strength of the various reinforcement tapes on the canopy. Table 1 lists the design lengths and rated strengths of the suspension lines. The canopy was constructed of 2.25 oz/yd², low permeability, nylon sailcloth, with the warp running parallel to the wing trailing edges. Main structural canopy seams were laid parallel to the trailing edges of the wing, joining leading-edge suspension line attachment points with adjacent keel line attachment points. These seams were reinforced with layers of nylon tape. All the outer edges and the keels of the canopy were reinforced with multiple layers of nylon tape. Highly stressed areas, such as suspension line attachments, were reinforced with semicircular or elliptical load-distribution patches fabricated from the basic canopy material. Where required, additional patch reinforcement was provided by overlaid radial tapes.

The initial large parawings were built and flown without the canopy ripstop tape matrix identified in Fig. 3. However, the not infrequent occurrence of localized cloth damage during initial parawing deployment and reefed inflation, sometimes followed by propagating cloth tears, led to the addition of the ripstop tapes.

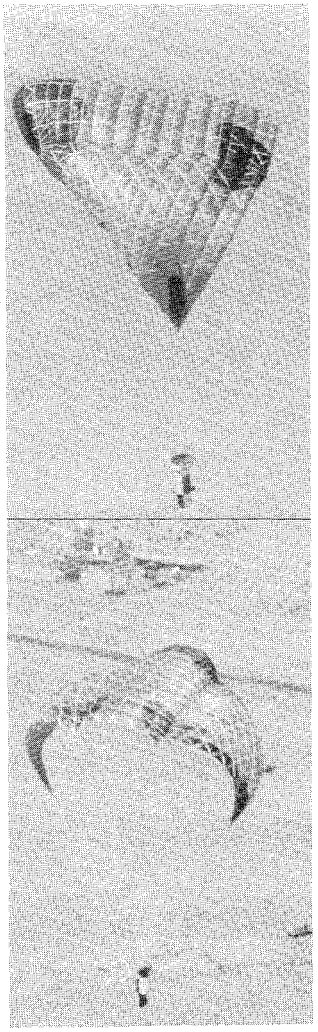

Fig. 1 4000 ft² twin keel parawing on bomb-type test vehicle.

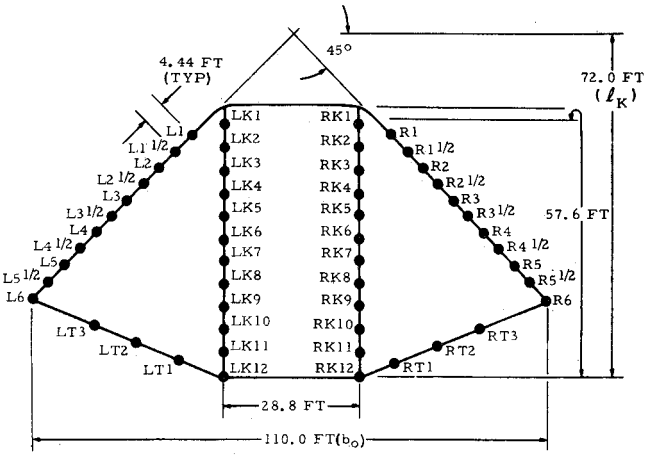

Fig. 2 Planform layout for large (4000 ft²) twin keel parawing.

Weight and Packed Volume

The weight of the large parawing shown in Fig. 3 was 330 lb. The corresponding weight of the parawing pack assembly, which included parawing, deployment bag, risers, line-stowage flutes, reefing system and loads instrumentation, was 370 lb. Packed volume of the large parawing was 11.75 ft³. In contrast, the weight of the small (400 ft²) parawing was about 26 lb, with a pack assembly weight of approximately 45 lb and a packed volume of 1.27 ft³.

Reefing Sequence

The parawing reefing sequence consisted of four reefed stages followed by the gliding configuration. Figure 4 shows, schematically, the arrangement of the various reefing lines and reefing cutters on the canopy. Figure 5 illustrates the canopy planform during each stage of reefed operation. The following paragraphs provide a stage-by-stage description of the reefing sequence.

Stage 1—The wing surface was reefed into three lobes by means of a separate reefing line on the periphery of each section of the wing (the center section and the two outboard sections). In addition, the wing trailing edges and the center section nose area were gathered with separate reefing lines. (Initial aerial tests of the parawing did not include the nose reefing. However, a load imbalance between stages 3 and 4, plus recurring cloth damage in the nose area of the wing, led to the addition of nose reefing.) Finally, suspension lines were shortened to the length of the tip suspension lines—the shortest suspension lines on the wing. Line lengths were

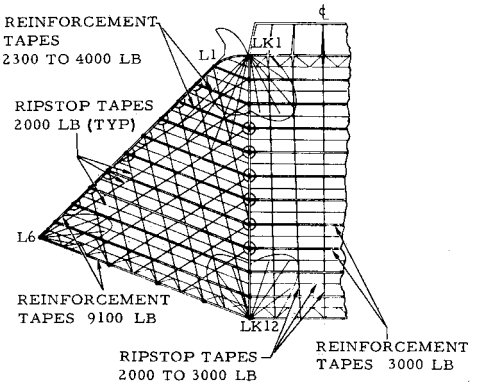

Fig. 3 Structural diagram for large parawing.

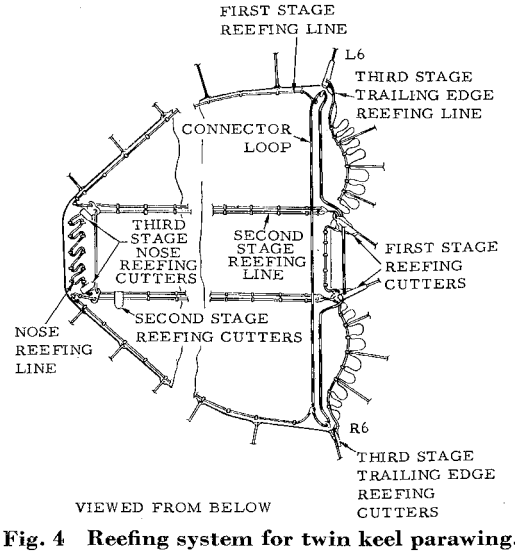

Fig. 4 Reefing system for twin keel parawing.

equalized to a) align the canopy inlets perpendicular to the airstream, b) eliminate loose suspension lines and their possible entanglement and/or abrasion during the deployment process, and c) reduce unequal suspension line loading. During stage 1 the parawing inflated to a three-lobed, balloon like shape, with three air inlets—one for each lobe—formed by the reefing lines, as shown in Fig. 5.

Stage 2—To establish stage 2, the reefing lines on the periphery of the outboard sections of the wing were severed. The parawing then inflated to the planform shape shown in Fig. 5, with the balloonlike center lobe, and outboard lobes similar in appearance to conventional parachutes.

Stage 3—To obtain stage 3, the reefing line on the periphery of the center section of the wing was severed. Figure 5 shows the planform of the wing in this stage, with and without nose reefing.

Stage 4—To achieve stage 4, the trailing edge gathering line and, if used, the nose gathering line, were severed. Thus in this stage all reefing lines were removed, with the wing inflating to the planform shown in Fig. 5.

Full open—For the final stage the suspension lines were released to their gliding flight lengths, and the wing made a transition to the gliding flight planform shown in Fig. 5.

In the test program the lengths of the first and second stage reefing lines were varied. The percent reefing was defined as

$$\% \text{ Reefing} = (l_{RL}/l_K) \times 100$$

In all of the tests conducted, the percent reefing in each of the three lobes was the same for any one test.

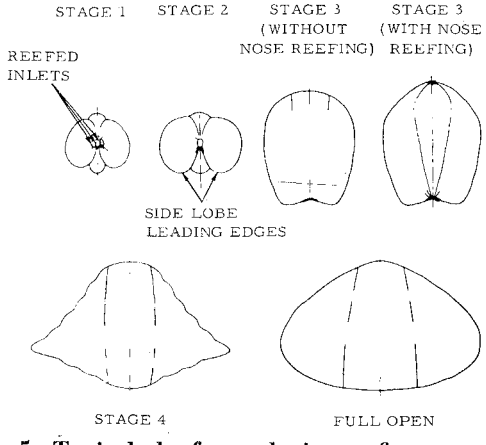

Fig. 5 Typical planforms during reefing sequence.

Deployment Performance

Total Loads

An objective in the program was to limit parawing total loads to 3G's or less for deployment in the dynamic pressure range of 30 to 100 psf, at altitudes from 3000 to 18,000 ft. In deployment tests of the parawing, a range of first and second stage reefing line ratios was evaluated. Figure 6 presents the actual, measured G-loads, stage by stage, for 15 tests of the large (4000 ft²) parawing. In these tests three different reefing ratios—14, 10 and 8%—were tested. Payload weights varied from 2900 to 6000 lb, and the dynamic pressure at parawing line stretch varied from 23 to 76 psf.

Figure 6 identifies that in order to maintain the stage 1 loads in the range of 3.0–3.5G's, a reefing percentage of 8% or less was required. It is worth noting that only the first stage G-loading was influenced significantly by the dynamic pressure at parawing initiation. Subsequent stages (second, third and fourth) were influenced significantly only by reefing ratio and by the reefing system changes, such as the use or nonuse of nose reefing. Figure 6 identifies the effect of nose reefing on the stage 3 and stage 4 G-loads. The filled symbols were the measured G-loads for parawings with nose reefing. Comparison of the tests with and without nose reefing clearly identifies how the addition of nose reefing served to balance the peak loads in these two stages.

Suspension Line Loads

In general, the reefing system utilized in the parawing test program resulted in nonuniform suspension line loading. This nonuniformity of line loading was both intrastage (unequal loading of individual suspension lines in a given reefing stage), and stage-to-stage (unequal loading of a given line from stage-to-stage). Figure 7 identifies both of these types of line load nonuniformity for the 11 line leading-edge parawing configuration. Figure 7 plots the line loads, expressed as a ratio of peak suspension-line load to peak-stage total load, for each line on the parawing and for each of the five deployment stages. The degree of line load nonuni-

Table 1 Large parawing suspension line design lengths and rated strengths

Suspension line	Design length, in.	Rated strength, lb
R1 and L1	803.5	5500
R1½ and L1½	796.6	3500
R2 and L2	786.2	5500
R2½ and L2½	777.6	4500
R3 and L3	769.0	5500
R3½ and L3½	747.4	4500
R4 and L4	730.1	5500
R4½ and L4½	699.8	3500
R5 and L5	673.9	5500
R5½ and L5½	636.8	3500
R6 and L6	521.0	5500
RK1 and LK1	842.4	4500
RK2 and LK2	855.4	4500
RK3 and LK3	851.0	4500
RK4 and LK4	842.4	4500
RK5 and LK5	842.4	4500
RK6 and LK6	842.4	4500
RK7 and LK7	833.8	4500
RK8 and LK8	833.8	4500
RK9 and LK9	829.4	4500
RK10 and LK10	820.8	4500
RK11 and LK11	803.5	4500
RK12 and LK12	824.3	5500
RT1 and LT1	925.0	3500
RT2 and LT2	925.0	3500
RT3 and LT3	808.0	3500

formity is evidenced by the fact that for the 4000 ft², 11 line leading-edge parawings, the ratio of total available suspension line strength to maximum design load was 4.9.

Canopy Deployment Damage

In the course of the large parawing flight tests, several tests resulted in canopy structural damage. Analysis of this damage identified four distinct failure modes. Of the four failure modes, three were relatively straightforward to isolate and correct. The fourth failure mode presented a problem, both in identifying the actual cause of the damage and in finding corrective measures which would completely eliminate the damage.

The first failure mode was structural damage in the central area of the wing leading edges during stage 2 reefed inflation. The damage was caused by high concentrated loads at the number 3 and 4 leading-edge line attachments, with inadequate canopy structure in the direction of primary loading. Corrective action included a beef-up of the line attachment locations, plus addition of the aforementioned 5 lines on each leading edge.

The second failure mode was damage in the form of cloth burns, holes and tears in the contoured nose section of the wing. The cloth burns and holes probably occurred during initial parawing deployment, due to cloth contact with the leading edge skirt band and/or the nose snubber lines.‡ The tears apparently occurred during third stage reefed inflation. Corrective action consisted of a) encasement of the nose snubber lines in cotton sateen sleeves, and b) separate reefing of the nose section of the wing.

The third failure mode was damage in the form of tears in the forward areas of the side lobes, between the leading edge band and the edge of the forward keel-line fan patch. The damage appeared to occur either during second or third stage reefed inflation and was adjudged to be due to local marginal canopy strength in the direction of loading. Corrective action consisted of extending further aft on the canopy the four reinforcing fan patch tapes.

The fourth failure mode and by far the most difficult to isolate and correct, was localized canopy cloth damage, often followed by propagating cloth tears. This damage occurred during initial canopy stretchout and first stage reefed inflation. It was apparently due to localized cloth abrasion and/or localized cloth overload during that interval when much of the canopy was relatively unconstrained and subjected to buffeting. (An unfortunate aspect of this problem was the fact that the lower reefing ratios increased the time interval in which the canopy was free to buffet. Thus, the lower reefing ratios needed to limit first stage loads increased the possibility of incurring canopy cloth damage.)

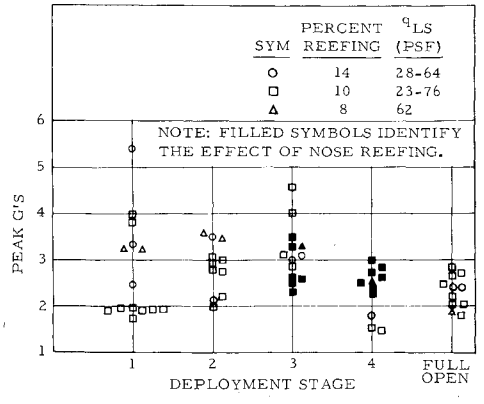

Fig. 6 Peak deceleration ratio vs deployment stage for the large parawing.

‡ Short, nylon lines which restrain the center section, nose area of the wing in its contoured shape.

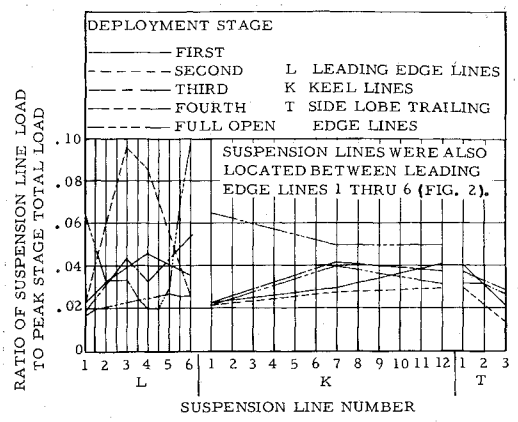

Fig. 7 Peak suspension line loading by stage.

The selected corrective action was the addition of a matrix of ripstop tapes to the parawing canopy to limit cloth tear propagation. While the corrective action did perform its design function, localized canopy cloth damage continued to occur in subsequent tests, with the amount of such damage increasing with increasing deployment dynamic pressure. Possible avenues for completely eliminating this type of damage include improved canopy cloth materials, a protective covering for the damage-susceptible cloth areas, selective canopy porosity to minimize buffeting following canopy stretchout, and alternate reefing schemes which provide better control of the canopy following its initial deployment.

It is significant to note that despite notable canopy damage incurred during parawing deployment in several flight tests of the large parawing, all the damaged wings did open and achieve a steady gliding configuration. This fact clearly demonstrates the positive opening characteristics and inherent opening reliability of the parawing device. Also, all damaged wings achieved a low vertical rate of descent prior to test vehicle touchdown. In fact, no test in the entire parawing program of 75 aerial drop tests resulted in loss of, or even major damage to a test vehicle—a record seldom equalled in aerodynamic decelerator development programs.

Gliding Flight Performance

In the course of the program, parawing gliding flight performance was evaluated as a function of such factors as rear keel-suspension line length, tip suspension line length and wing loading. On the basis of previous investigations, the rear keel suspension lines (LK12 and RK12) and the tip suspension lines (L6 and R6) were selected for pitch and directional control. Both sets of lines were varied individually and in combination to determine their useful range of travel and the effects of varying their lengths on gliding performance.

Straight Gliding Flight

Figures 8 and 9 summarize the variation of L/D, C_L and C_D as a function of rear keel setting (where rear keel setting refers to the ratio of the rear keel-line length to keel length). The data in Fig. 8 compare wind-tunnel L/D performance of small parawings with free-flight performance of both small and large parawings. Figure 9 compares wind-tunnel measured C_L and C_D for small parawings with free-flight values for large parawings (no C_L and C_D data were obtained during small parawing free flight tests). The range of rear keel settings shown in Figs. 8 and 9 represents the range in which the rear keel-line length could be varied while maintaining

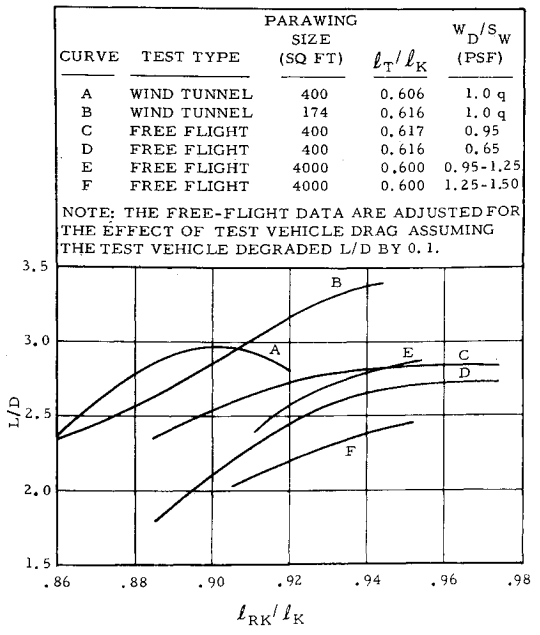

Fig. 8 Free flight and wind tunnel L/D data.

stable flight and/or stable canopy inflation. The lowest rear keel setting was determined by wing stall. Figure 8 shows that the free-flight L/D performance was reasonably consistent between the small and the large parawings. However, the parawing wind-tunnel L/D performance was significantly higher than the free-flight performance, even when the data were adjusted for the effect of test vehicle drag. The most probable explanation for this variation is differences in the inflated shape of the wing as a result of the method of mounting the wing in the wind tunnel, compared with the method of wing attachment to the free flight test vehicles. It may be noted on Fig. 9 that C_L and C_D values measured in free flight were correspondingly lower than those measured in wind-tunnel tests.

Figure 8 shows that rear keel-line retraction could only reduce L/D on the large parawings by an increment of approximately 0.5 from the maximum L/D. Thus, rear keel line control is considered ineffective as a means for adjusting the system glide path during a landing maneuver, due to the narrow range of variability available. Figure 10 summarizes the effect of tip setting on L/D for large parawing free-flight

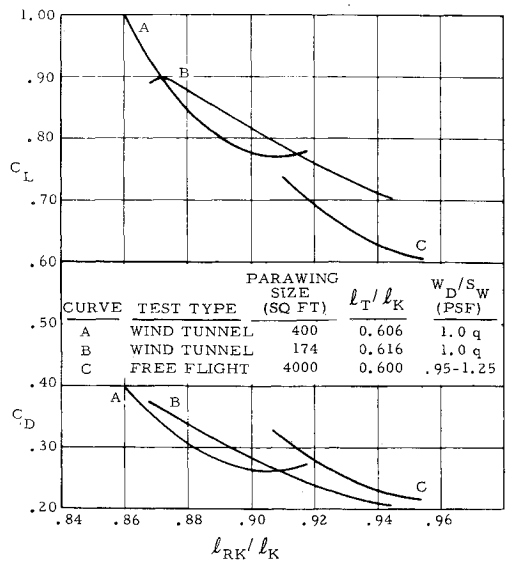

Fig. 9 Free flight and wind tunnel C_L and C_D data.

tests. While there were measurable changes in the L/D level from test to test, due primarily to wing loading, no significant change in L/D was obtained with changes in tip setting. Also shown on Fig. 10 is a curve of L/D vs tip setting measured on small parawings in the wind tunnel. In contrast to the free-flight data, the tunnel data indicated a significant change in L/D with tip setting. The curve shows that L/D increased by 0.6 when the tip lines were retracted from $0.63l_K$ to $0.60l_K$. Again, this difference between free-flight and wind-tunnel performance may be attributable to the method of wing mounting in the wind tunnel, compared with the method of wing attachment to the free-flight test vehicles. In any event, the large parawing free-flight tests showed that tip setting, as well as rear keel setting, is ineffective as a means for varying the parawing/payload glide path. Varying the parawing tip setting in free-flight tests established that the usable range for this setting was from 0.57 to 0.64. Setting less than 0.57 resulted in wing stall. Settings greater than 0.64 resulted in collapse of the wing leading edges.

Figure 11 summarizes the effect of wing loading on parawing L/D performance, measured both in the wind tunnel and in free flight. As shown in Fig. 11, L/D generally decreased with increasing wing loading. No definitive explanation for this behavior was obtained during the program. However, a possible explanation for this characteristic is that the higher tensile forces associated with increased wing loading distorted the parawing canopy to a less favorable shape. Extensive parawing wind-tunnel tests conducted by the Langley Research Center over a wide range of canopy loadings (dynamic pressures) have shown that maximum L/D can be reasonably well maintained by successive adjustment of the parawing suspension line rigging. However, data from the large parawing free-flight tests showed that varying the tip setting and/or the rear keel setting could not alone compensate for the effect of wing loading on L/D performance.

Directional Control

Directional control of the parawings was obtained by differentially changing the length of the tip suspension lines, which caused the wing to turn in the direction of the shorter tip line. The effect of the differential tip setting was similar to the effects of tip mounted rudders located above the c.g. on a flying wing aircraft. The portion of the parawing side panels in the vertical plane acted in a manner similar to these rudders. Retracting a tip control line deflected the trailing edge of the associated side panel. This deflection generated a side force above the c.g. which resulted in a rolling moment, and a drag increase outboard of the c.g., which resulted in a yawing moment. Both of these moments were favorable, relative to the desired direction of turn. Reference 3 gives experimental values of lateral, directional and longitudinal derivatives for the twin keel parawing.

With the parawing attachment geometry used in the test program, turn rate was found to be a linear function of the difference in length between the tip suspension lines. The maximum differential tip setting (δ_T/l_K) for effective turn control was found to be 0.07, with the aforementioned limita-

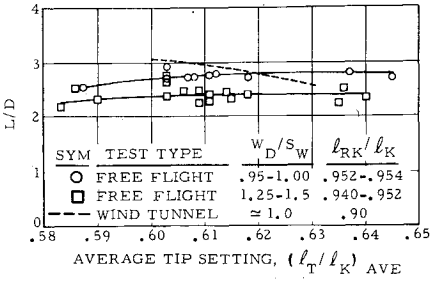

Fig. 10 L/D vs average tip setting.

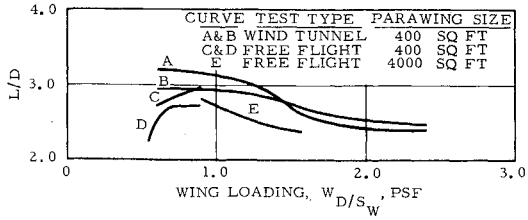

Fig. 11 Summary of parawing L/D vs wing loading.

tion that the shorter tip line length be not less than $0.57l_K$, and the longer tip line length be not more than $0.64l_K$. For a given size wing and tip control setting, turn rate was found to be proportional to wing loading to the 1.564 power.

Figure 12 shows parawing turn rate data from both small and large parawing free-flight tests. The data show that turn rate ($\dot{\psi}$) was a function of differential tip setting (δ_T/l_K), wing loading (W_D/S_W), and wing size as characterized by keel length (l_K). In Fig. 12 the normalized turn rate ($\dot{\psi}/\delta_T/l_K$) is plotted vs the ratio of wing loading to keel length. The resulting curve on Fig. 12 can be expressed as

$$\dot{\psi}/(\delta_T/l_K) = 3.248[(W_D/S_W)/l_K]^{1.564} \times 10^5$$

In practical terms, the large parawings had quite adequate turn capability. With the maximum differential tip setting of 0.07, the large wings had a turn rate capability of 40 deg/sec at a wing loading of 1.25 psf and 53 deg/sec at a wing loading of 1.50 psf. At comparable wing loadings the small (400 ft²) parawings had turn rate capabilities of 245 deg/sec and 325 deg/sec, respectively, for the maximum differential tip setting of 0.07. This level of turn rate capability was excessive. In controlled, free-flight tests with the small wings, care was required by the ground controller to avoid these high turn rates, particularly near the ground. The high turn rates caused the payload to move in a wide coning motion which would have resulted in damage to the payload at touchdown.

Conclusions

Based on the results of the parawing program, several conclusions can be drawn. First, the program demonstrated that large parawings can be built, deployed at high speed, and subsequently brought to a configuration for controlled, gliding flight. Second, the parawing exhibited very positive opening characteristics, even after having incurred notable canopy damage—an important factor for any decelerator being considered for spacecraft application. Third, the tests showed that the parawing can be reliably multistage reefed to provide 3–3.5G load levels and stable operation during the deployment process. Fourth, free-flight performance of the parawings was very satisfactory. In general, the parawing in free flight behaved in a manner similar to a low-speed, glider-type airplane. With the proper tip and rear keel control-line setting, the wing maintained a solidly inflated condition, with no tendency to stall during turning maneuvers or when encountering turbulent air flight conditions. Also, when trimmed for straight flight, the wing maintained a straight flight course without additional control inputs. Turn control capability on the parawings flown was more than adequate. L/D capability in the range of 2.5 to 2.75 was consistently demonstrated. However, no appreciable L/D modulation capability was possible, using either rear keel or tip line controls. This limitation would influence the landing approach techniques which would be used with a parawing landing system.

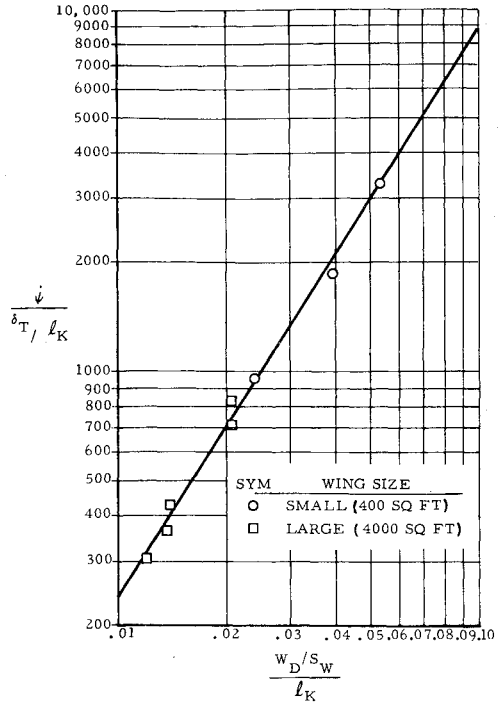

Fig. 12 Normalized turn rate as a function of wing loading and reference keel length.

The most significant problem encountered in the program was the occasional occurrence of localized canopy cloth damage during initial parawing deployment. The exact cause of this damage was not determined, and the corrective action taken to overcome the problem was not completely satisfactory. Although troublesome, this damage did not seriously compromise parawing flight performance. Analysis and preliminary tests indicate that improved reefing techniques, possibly coupled with controlled canopy porosity, could provide the means for overcoming this problem. Such improved reefing techniques could also provide more uniform suspension line loading—the key to a lightweight parawing design.

Finally, the technology developed in this program indicates that parawings for landing payloads in excess of 6000 lb weight can be developed successfully. More complete details of the parawing technology program are contained in Refs. 4 and 5.

References

[1] Naeseth, R. L. and Fournier, P. G., "Low Speed Wind Tunnel Investigation of Tension Structure Parawings," TN-D-3940, June 1967, NASA.

[2] Naeseth, R. L., "Low-Speed Wind-Tunnel Investigation of a Series of Twin Keel All Flexible Parawings," LWP-347, January 1967, NASA.

[3] Ware, G. M., "Wing-Tunnel Investigation of the Aerodynamic Characteristics of a Twin-Keel Parawing," TN D-5199, May 1969, NASA.

[4] Linhart, E. M. and Buhler, W. C., "Wind Tunnel and Free Flight Investigation of All-Flexible Parawings at Small Scale," CR-66879, June 1969, NASA.

[5] Moeller, J. H., Linhart, E. M., Gran, W. M., and Parson, L. T., "Free Flight Investigation of Large All Flexible Parawings and Performance Comparison With Small Parawings—Final Report," CR-66918, March 1970, NASA.